UNIVERSIDAD
NACIONAL
DE COLOMBIA
S E D E B O G O T Á
FACULTAD DE CIENCIAS
DEPARTAMENTO DE GEOCIENCIAS
RESEARCH GROUP IN GEOPHYSICS

PETROLOGY

Petrologic significance of Fe-rich staurolite in pelitic schists of the Silgará Formation, Santander Massif

Carlos Alberto Ríos R.[1*], Oscar Mauricio Castellanos A.[2]

[1*]. Escuela de Geología, Universidad Industrial de Santander, Bucaramanga, Colombia, e-mail: carios@uis.edu.co

[2]. Programa de Geología, Universidad de Pamplona, Colombia

ABSTRACT

Medium grade metapelites of the Silgará Formation at the Santander Massif (Colombian Andes) have been affected by a medium-pressure/high-temperature Barrovian type of metamorphism, developing a sequence of metamorphic zones (biotite, garnet, staurolite and sillimanite). These rocks record a complex tectono-metamorphic evolution and reaction history. Metapelitic rocks from the staurolite zone are typically foliated, medium- to coarse-grained, pelitic to semipelitic schists that contain the mineral assemblage biotite + garnet + staurolite ± kyanite; all contain muscovite + quartz + plagioclase with minor K-feldspar, tourmaline, apatite, zircon, epidote, calcite, and Fe–Ti oxides. Field and microscopic evidences reveal that Fe-rich staurolite in pelitic schists is involved in several chemical reactions, which explains its formation and transformation to other minerals, which are very important to elucidate the reaction history of the Silgará Formation metapelites.

Significado Petrológico de Estaurolita Rica en Fe en Esquistos Pelíticos de la Formación Silgará, Macizo de Santander

RESUMEN

Medium grade metapelites of the Silgará Formation en el Macizo de Santander (Andes Colombianos) han sido afectadas por un metamorfismo de tipo Barroviense, el cual se ha producido en condiciones de media presión y alta temperatura, desarrollando una secuencia de zonas metamórficas (biotita, granate, estaurolita y silimanita). Estas rocas registran una evolución tectono-metamórfico e historia reacción compleja. Las metapelitas de la zona de la estaurolita están representadas por esquistos pelíticos a semipelíticos de grano medio a grueso típicamente foliados que contienen la paragénesis mineral biotita + granate + estaurolita ± cianita; todos contienen moscovita + cuarzo + plagioclasa con menor feldespato potásico, turmalina, apatito, zircón, epidota, calcita, y óxidos de Fe-Ti. Evidencias de campo y microscópicas revelan que la estaurolita rica en Fe en esquistos pelíticos se involucró en varias reacciones químicas a partir de las cuales esta se formó o transformó a otra fase mineral, lo cual es muy importante para dilucidar la historia de reacción de los metapelitas de la Formación Silgará.

1. Introduction

The metamorphic history of the Santander Massif is well documented by Ríos and co-workers (e.g., Ríos et al., 2003; García et al., 2005; Ríos et al., 2005; Castellanos et al., 2008), and only a brief overview of events is presented here. Two distinct geological domains constitute the crystalline basement of the Santander Massif (Castellanos et al., 2008): (1) the deformed and metamorphosed rocks of the Precambrian Bucaramanga Gneiss Complex, the Lower Paleozoic Silgará Formation and the Ordovician Orthogneiss and (2) a Triassic-Jurassic post-orogenic magmatism with calc-alkaline affinity which developed after the Paleozoic syn-orogenic magmatism with alkaline affinity (e.g., Goldsmith et al., 1971; Banks et al., 1985; Dörr et al., 1995; Ordoñez, 2003). The metamorphic rocks of the Silgará Formation in the Santander Massif (Figure 1) were metamorphosed to upper amphibolites facies during the Caledonian orogeny, developing a sequence of metamorphic zones (biotite, garnet, staurolite and sillimanite) that defines the regional thermal structure. The Silgará Formation consists of predominantly metapelitic to semipelitic rocks with interlayered mafic rocks on scales ranging from a few centimeters to several meters. These rocks have been intruded by granitoids and gabbros during the Triassic-Jurassic (Goldsmith et al., 1971). However, the occurrence of a thermal event superimposed to the regional metamorphism should be considered, which is evidenced by the emplacement of granitoids associated to a late magmatism of the Silurian Fammatinian minor orogenic event proposed by Mantilla et al. (2015). Metamorphic rocks of the Silgará Formation show evidence of a complex metamorphic history characterized by crustal thickening during heating and a regional retrograde metamorphism after the peak metamorphic temperature (Ríos et al., 2003). The rocks of interest in this study correspond to staurolite-bearing metapelitic rocks, which form part of the Barrow's staurolite zone, and record conditions of 590–612 ºC and 6.6–7.5 kbar (Ríos et al., 2003). Garnet can grow from a variety of reactions over a large range of P-T conditions and so the recognition of multiple phases of growth in rocks of different compositions is well documented (e.g., Bell and Welch, 2002). In contrast, staurolite forming reactions typically have a lower variance than garnet forming reactions (Sanislav and Shah, 2010). Multiple steps of staurolite growth in metapelitic rocks of the Silgará Formation with little or no change in bulk composition can be recognized, which, according to Sanislav and Shah (2010) has considerable implications for the common assumption that mineral reactions are controlled by the whole rock bulk chemistry. They demonstrate that mineral reactions are controlled by sites of strain localization rather than whole rock reaction. In this work we document the occurrence of Fe-rich staurolite in pelitic schists of the Silgará Formation (Santander Massif). From the staurolite's chemistry, in combination with textural observations, phase equilibria, and evidence for early crystallization and later destruction of ordinary staurolite, we infer that this metamorphic unit has undergone a polymetamorphic history.
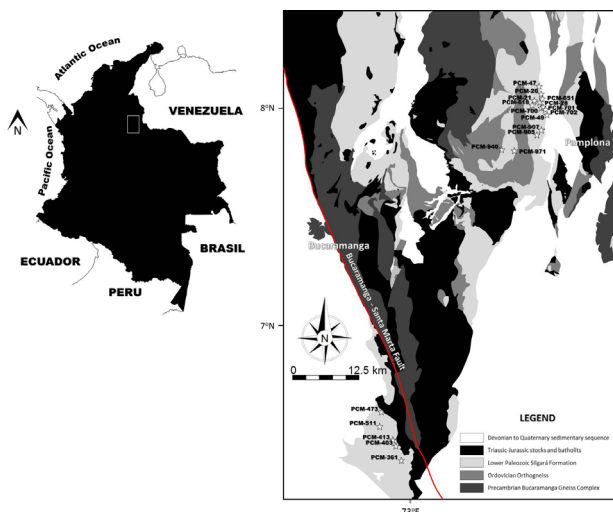
2. Field sampling and analytical methods

A research team from the University Industrial de Santander was involved in reconnaissance fieldwork on the Santander Massif. Fieldwork was primarily focused on localities with staurolite in pelitic schists from the Silgará Formation as previously reported (Ríos et al., 2003; García et al., 2005) and the sampling strategy focused on taking staurolite-bearing samples from several outcrops. Detailed petrographic studies of thin sections were carried out on all specimens using a trinocular Nikon (Labophot2-POL) transmitted light microscope of the School of Geology, University Industrial de Santander. Mineral abbreviations are after Kretz (1983). Electron microprobe analyses were performed using a JEOL JXA 8800M electron probe microanalyzer at the Research Center for Coastal Lagoon Environments, Shimane University (Japan), under the following analytical conditions: accelerating voltage 15 kV and probe current 2.5 x 10^{-8} Å. Data acquisition and reduction were carried out using ZAF correction procedures. Natural and synthetic minerals were used as standards. Mineral compositions were determined by multiple spot analyses.

3. Field occurrence

The metamorphic rocks of the Silgará Formation display a well-developed schistosity and has been divided by Ríos et al. (2003) into dominantly metapelitic (to semipelitic) and with minor intercalations of metamafic rocks (Figure 2). The lithology changes northeastward from quartz-rich pelitic schists (southwest) to feldspar-rich semipelitic schists (northeast). The staurolite zone can easily be recognized because it forms a wide zone and because staurolite only grows within the most pelitic horizons of the Silgará Formation. Pelitic schists from this metamorphic zone have a lustrous silvery aspect and are coarser grained than those from the garnet zone. Staurolite forms honey-brown large prismatic porphyroblasts which quite frequently reach up to 1.2 cm across and 12 cm in length, elongated along the schistosity and usually displaying reaction rims. It is usually abundant along with garnet, particularly in the transition between the garnet and staurolite metamorphic zones.
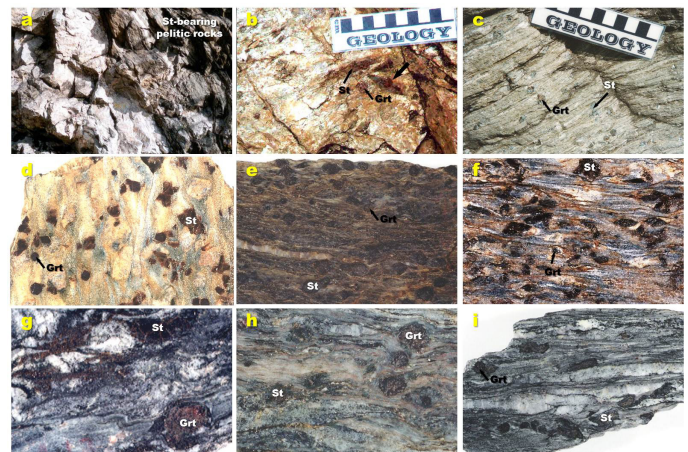

Figure 2. Field and hand-specimen photographs of staurolite-bearing metapelitic rocks of the Silgará Formation at the Santander Massif. (a) Outcrop of metapelitic rocks interlayered with quartzites. (b) Pelitic schist displaying a tabular geometry and schistosity. (c) Close-up of an outcrop showing the occurrence of a staurolite-bearing pelitic schist. (d)-(i) Several examples of the occurrence of garnet-staurolite mica schists; the luster is from large muscovite grains; the equidimensional porphyroblasts are garnet; untwinned staurolite porphyroblasts are larger and darker than garnet. The orange-reddish color of muscovite is due to Fe-oxide/hydroxide staining.

Figure 1. Generalized geological map of the Santander Massif modified after Ward et al. (1970, 1973). Open stars indicate the location of staurolite-bearing metapelitic rocks.

4. Petrography

Staurolite-bearing pelitic schists are typically foliated, medium- to coarse-grained, that contain graphite and Fe-Ti oxides. In general, they are represented by the mineral assemblage muscovite + biotite + quartz + plagioclase + garnet + staurolite ± kyanite. They also contain minor K-feldspar, tourmaline, apatite, zircon, epidote, calcite, and Fe–Ti oxides). They display a well-developed schistosity defined by the preferred orientation of muscovite and biotite flakes and crystals of graphite and Fe-Ti oxides. Biotite is not only present as small flakes underlying the planar structure but also as lozenge-shaped crystals which represent early porphyroblasts and their asymmetry is sometimes useful to determine sense of shear. A last generation of biotite appears as undeformed crystals with their cleavage randomly oriented to the schistosity and can be interpreted as due to a postkinematic thermal event. Quartz and plagioclase form domains between the mica-domains. Garnet, usually equigranular, occurs as euhedral to subhedral large porphyroblasts (up to 1.2 cm diameter), with cores frequently rich in minute inclusions of quartz, plagioclase, graphite and Fe-Ti oxides, and their rims are poorer in inclusions. Most of the garnets do however contain inclusion trails of quartz and opaque minerals. The inclusion trails either form straight lines or sigmoidal structures within the garnet poikiloblasts. The garnets with straight inclusion trails can be restricted to the upper structural part of the staurolite zone, whereas the garnets with sigmoidal inclusion trails appear in the lower structural part of the staurolite zone. Depending on their structural position, the garnets are thus either pre-, syn or post-tectonic with respect to D_3 (S_3). Pre-tectonic garnet develops shattered and partially chloritized porphyroblasts, with muscovite and ilmenite parallel to the rock's dominant foliation (S_e) wrapping around garnet and mica and quartz occurring in strain shadows. Garnet sometimes occurs as elongated grains parallel to S_e. Inclusion patterns in syn-tectonic garnet define an internal foliation (S_i), usually discordant to S_e, and sometimes developing a pattern of sigmoidal inclusions. Post-tectonic garnet has overgrown S_i or S_e, with quartz and ilmenite as the main inclusions. Another characteristic texture is large web-like garnet crystals that contain so many quartz inclusions that the quartz predominates. Staurolite commonly forms euhedral poikiloblastic porphyroblasts with elongated prismatic shapes of various aspect ratios (1.2 cm across), which can contain inclusion trails that preserve earlier fabrics. It grew late after garnet. It displays a moderate preferred orientation of elongate crystals (contain quartz and ilmenite inclusions parallel to S_e) parallel to S_e, indicating that it formed during the late regional metamorphism. On the other hand, in the direction of shear, staurolite porphyroblasts with high aspect ratios tend to lie with their long axis parallel to S_e. Straight inclusion trails oriented at various angles with respect to S_e reveals that staurolite porphyroblasts rotated with respect to rock's dominant foliation. Various angles of the internal foliation (S_i), represented by straight quartz inclusion trails, with the external foliation (S_e) indicate that rotation of staurolite porphyroblasts was not uniform and depended on their aspect ratios and their orientation in space with respect to the kinematic frame of the bulk flow prior to the onset of deformation (e.g., Johnson, 2009; Mezger, 2010). Staurolite overgrew mica- and quartz-feldspar-domains, which have been preserved as inclusion-poor and inclusion-rich zones, respectively, that give porphyroblasts a striped appearance (Mezger, 2010). It also shows sigmoidal patterns of inclusions that indicate syn-kinematic crystallization. However, it can be also oriented across S_e indicating post-kinematic crystallization. Both generations of staurolite are rich in inclusions of quartz, Fe-Ti oxides, and minor graphite. Staurolite is commonly retrogressed to sericite, although chlorite is also a common retrograde alteration product of this mineral. Small-scale folding of the schistosity planes has produced a crenulation cleavage, accompanied by segregation of quartz into layers. Deformation structures in the mylonitic rocks from the staurolite zone is very interesting as it reveals that these rocks have undergone two major phases of ductile deformation showing opposite sense of shear. The oldest phase of deformation is preserved as inclusion trails within the poikiloblastic garnet or staurolite porphyroblasts, and shear sense criteria for this phase are given by the syn-tectonic sigmoidal garnet or staurolite. From the whole story of polymetamorphism it seems that kyanite belongs to the early events with deformation and andalusite and sillimanite (fibrolite) to the late (contact) metamorphism. These rocks frequently contain evidence of retrograde metamorphism, involving hydration processes, including partial replacement of garnet, biotite and staurolite by chlorite, staurolite by muscovite and plagioclase and staurolite by sericite. Figure 3 illustrates the main petrographical aspects of the investigated staurolite-bearing pelitic schists.
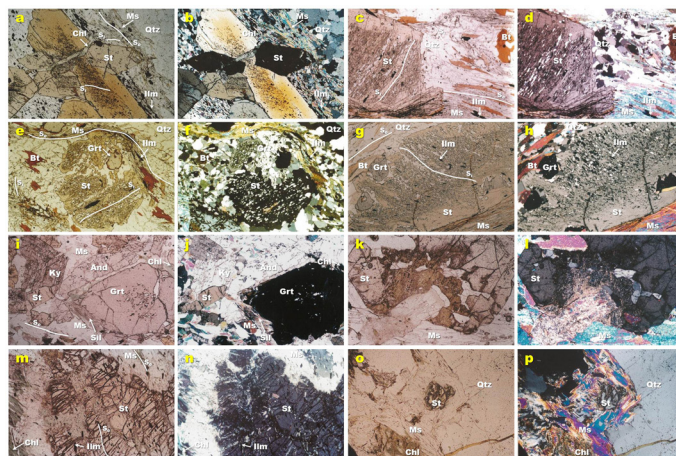

Figure 3. (a)-(b) Staurolite in a muscovite-biotite schist, displaying parallel extinction, one cleavage parallel to its length, and characteristic pale to darker golden yellow pleochroism; this example has a twin, highlighted by different color and birefringence caused by its different orientation. (c)-(d) Staurolite showing inclusion patterns defining Si discordant to Se, and inclusion-free rim. (e)-(h) Relics of garnet included in late staurolite porphyroblasts. (i)-(j) Occurrence of staurolite in a garnet-staurolite schist containing kyanite, andalusite and sillimanite. (k)-(p) Resorption of staurolite by sericite and muscovite, developing reaction rims around staurolite.

5. Staurolite crystal chemistry

Representative analyses of staurolite are given in Table 1. Staurolite is Fe rich (X_{Fe} = 0.68-0.90), with 9.22-14.97 wt.% FeO and 0.71-2.42 wt.% MgO, and characteristically higher in X_{Fe} than coexisting minerals, and contains up to 0.81 wt.% TiO_2 and up to 3.70 wt.% ZnO. The ZnO content in staurolite reveals the highest values (2.37-3.70 wt.% ZnO) for samples PCM-49 and PCM-361, and the lowest values (0.05 wt.% ZnO) for samples PCM-701 and PCM-905.

Table 1. Representative chemical compositions of staurolite-bearing pelitic rocks of the Silgará Formation at the Santander Massif.

Sample No.	PCM-20	PCM-21	PCM-28	PCM-47	PCM-49	PCM-361	PCM-403	PCM-413	PCM-473	PCM-511	PCM-618	PCM-651	PCM-700	PCM-701	PCM-702	PCM-905	PCM-907	PCM-940	PCM-971
Weight %																			
SiO_2	26.95	27.94	26.45	27.86	27.74	27.02	27.22	27.34	27.26	27.20	26.55	27.56	26.44	26.97	28.62	27.31	27.11	26.54	26.68
TiO_2	0.46	0.46	0.64	0.52	0.40	0.44	0.60	0.64	0.69	0.67	0.52	0.63	0.64	0.70	0.55	0.58	0.52	0.81	0.60
Al_2O_3	54.44	52.81	53.75	53.17	52.77	54.43	54.52	52.10	54.87	55.13	54.48	52.68	53.64	53.78	51.85	52.97	53.33	53.76	53.17
FeO*	13.43	12.79	14.03	13.80	9.22	11.86	13.13	13.84	12.49	11.89	13.19	14.50	13.94	14.76	14.97	13.79	13.84	13.16	14.05
MnO	0.02	0.50	0.06	0.05	1.24	0.14	0.23	0.00	0.17	0.71	0.01	0.05	0.01	0.03	0.03	0.29	0.41	0.64	0.15
MgO	2.42	2.27	1.87	1.81	2.39	0.94	1.11	2.23	1.00	0.71	1.21	1.55	0.92	1.52	1.45	1.94	1.89	1.54	1.28
CaO	0.03	0.00	0.00	0.00	0.02	0.02	0.00	0.00	0.00	0.00	0.00	0.00	0.00	0.00	0.02	0.02	0.00	0.01	0.00
Na_2O	0.02	0.00	0.03	0.02	0.14	0.11	0.01	0.05	0.05	0.05	0.08	0.01	0.01	0.00	0.00	0.03	0.00	0.07	0.07
K_2O	0.01	0.03	0.03	0.03	0.03	0.07	0.00	0.03	0.02	0.02	0.04	0.02	0.01	0.06	0.03	0.03	0.03	0.06	0.04
ZnO	0.08	0.61	0.56	0.15	3.70	2.37	1.10	0.71	1.70	0.85	1.34	0.50	0.62	0.05	0.12	0.05	0.30	1.16	1.36
Cr_2O_3	0.01	0.04	0.04	0.04	0.03	0.01	0.02	0.00	0.02	0.01	0.04	0.08	0.04	0.05	0.05	0.06	0.04	0.05	0.00
Total	97.87	97.44	97.46	97.44	97.67	97.40	97.93	96.94	98.28	97.24	97.47	97.58	96.27	97.92	97.67	97.07	97.47	97.81	97.39
Numbers of ions on the basis of 23 oxygens																			
Si	3.738	3.896	3.710	3.884	3.876	3.783	3.786	3.852	3.777	3.787	3.720	3.862	3.748	3.763	3.999	3.831	3.795	3.717	3.761
Al^{IV}	0.262	0.104	0.290	0.116	0.124	0.217	0.214	0.148	0.223	0.213	0.280	0.138	0.252	0.237	0.001	0.169	0.205	0.283	0.239
sum T	4.000	4.000	4.000	4.000	4.000	4.000	4.000	4.000	4.000	4.000	4.000	4.000	4.000	4.000	4.000	4.000	4.000	4.000	4.000
Al^{VI}	8.638	8.575	8.596	8.620	8.565	8.763	8.721	8.504	8.739	8.835	8.715	8.561	8.711	8.607	8.538	8.587	8.593	8.591	8.596
Cr	0.001	0.005	0.004	0.005	0.003	0.001	0.002	0.000	0.002	0.002	0.004	0.009	0.005	0.006	0.005	0.006	0.005	0.006	0.000
Ti	0.048	0.048	0.068	0.054	0.042	0.046	0.063	0.068	0.072	0.070	0.055	0.066	0.069	0.073	0.057	0.061	0.055	0.086	0.064
Fe^{2+}	1.558	1.491	1.646	1.609	1.077	1.388	1.526	1.630	1.447	1.385	1.545	1.698	1.653	1.722	1.749	1.617	1.620	1.542	1.657
Mn	0.002	0.059	0.007	0.006	0.146	0.017	0.027	0.000	0.020	0.084	0.001	0.005	0.001	0.004	0.003	0.035	0.048	0.076	0.017
Zn	0.008	0.062	0.058	0.015	0.382	0.245	0.113	0.073	0.174	0.088	0.139	0.051	0.065	0.005	0.012	0.005	0.031	0.120	0.141
Mg	0.500	0.471	0.391	0.377	0.498	0.195	0.230	0.468	0.207	0.147	0.253	0.325	0.194	0.316	0.301	0.406	0.394	0.322	0.268
sum Y	10.756	10.712	10.770	10.687	10.712	10.656	10.683	10.744	10.661	10.609	10.712	10.715	10.698	10.733	10.666	10.718	10.746	10.741	10.744
Ca	0.004	0.000	0.000	0.000	0.003	0.003	0.000	0.000	0.000	0.000	0.001	0.000	0.000	0.000	0.003	0.003	0.000	0.001	0.000
Na	0.005	0.000	0.009	0.005	0.039	0.030	0.001	0.014	0.014	0.014	0.021	0.002	0.003	0.000	0.000	0.008	0.001	0.019	0.019
K	0.002	0.005	0.006	0.005	0.005	0.012	0.000	0.006	0.004	0.004	0.007	0.004	0.001	0.011	0.008	0.005	0.005	0.011	0.007
sum X	0.012	0.005	0.015	0.009	0.047	0.044	0.001	0.019	0.018	0.018	0.028	0.006	0.004	0.011	0.008	0.015	0.006	0.031	0.027
Total	14.767	14.716	14.784	14.696	14.759	14.701	14.684	14.764	14.679	14.627	14.740	14.721	14.702	14.744	14.674	14.733	14.752	14.772	14.771
*Total Fe as FeO																			
X_{Fe}	0.76	0.76	0.81	0.81	0.68	0.88	0.87	0.78	0.87	0.90	0.86	0.84	0.89	0.84	0.85	0.80	0.80	0.83	0.86

In general, staurolite shows slight compositional variation, which can be related to coexisting minerals, becoming more Fe rich toward the rim of individual porphyroblasts, although with no appreciable crystal to crystal variations in chemical composition (Figure 4).
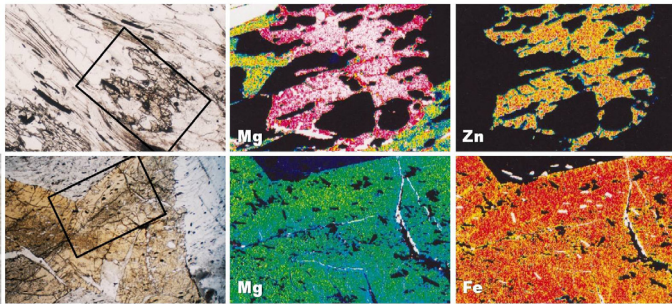

Figure 4. Textural features of skeletal (above) and twinned (below) staurolite and the Mg and Zn color maps of the skeletal staurolite and Mg and Fe color maps of the twinned staurolite.

An idealized formulae of staurolite, such as $(Fe^{2+},Mg,Zn)^{VI}_2(Al,Fe_3+,Ti)^{VI}_9O_6[(Si,Al)O_4]_4(O,OH)_4$ does not consider the complex crystal chemistry of this metamorphic mineral (Smith, 1968). Griffen and Ribbe (1973) inferred from a statistical study of staurolite analyses that Fe, Mg and Al are each distributed over both the tetrahedral Fe and the octahedral Al sites, with Fe preferring the tetrahedral occupancy and Mg and Al the octahedral occupancy. Therefore, Fe and Mg are not related by the simple one-for-one substitution scheme implied by the formulae above. Staurolite analyses were normalized on a 46-oxygen basis, assuming 4 H per formula unit. On this basis the total of Mg+Fe cations is unusually high, up to 4.197, which is lower than results reported in previous studies (e.g., Gritren and Ribbe, 1973; Ward, 1984). Cation totals in the range 29.348-29.569 are similar to those obtained by Gritren and Ribbe (1973) and lower than unusually high cation totals reported by Ward (1984). Figure 5 illustrates plots of Mg+Fe vs. Al, and Mg+Fe vs. Al′, where Al′ is Al+Si-8 (that is, Al cations per unit cell after subtracting Al to fill up the tetrahedral Si site to 8). Different to what is suggested by Ward (1984), there is no strong correlation after this adjustment, and therefore we cannot assume that Al fills up the Si site to essentially full occupancy (Griffen et al., 1982). The extent of the adjustment is considerable because of the variable and low Si content. The high Si content (7.420-7.997) compared with values

(7.374-7.538) reported by Ward (1984) reveals a high silica activity of the rock, which is manifested by the occurrence of abundant quartz. There is no good correlation of Mg+Fe vs. Al′ (with considerable variation of Mg), and, therefore, we cannot support the idea of an important (Mg,Fe) = Al substitution in the octahedral sites as revealed by Gritren and Ribbe (1973). Staurolite is the only common silicate phase, which can incorporate significant amounts of Zn in rocks of the amphibolite facies. Zn substitutes for tetrahedrally coordinated divalent Fe (Deer et al., 1982), and partitions strongly into staurolite due to the lack of other suitable cation sites. At higher metamorphic grade, as staurolite begins to react out, Zn is increasingly concentrated in the remaining staurolite.
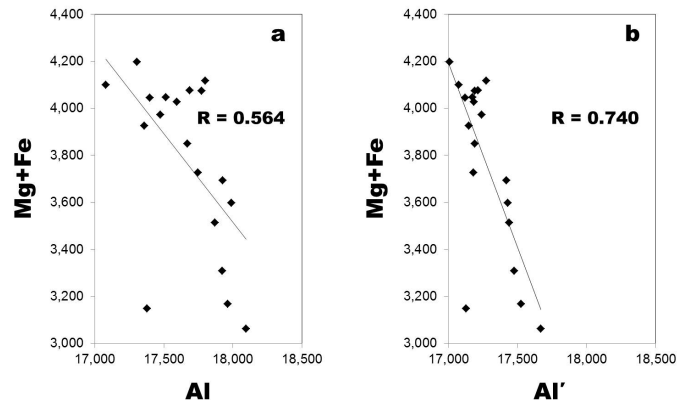

Figure 5. Mg+Fe vs. Al (left) and Mg+Fe vs. Al′ (right) plots for staurolite from pelitic rocks. Least squares regression lines are shown.

6. Petrologic significance

Metapelitic rocks containing staurolite commonly occur in medium-P regional metamorphism in the staurolite zone of the amphibolite facies, where staurolite is associated with almandine, muscovite, quartz and kyanite. However, staurolite-pelitic schists are not always encountered even though the P-T conditions lie within the stability field of staurolite, which led several petrologists to suggest that the bulk chemical composition plays an important role in the formation of staurolite in pelitic schists that are rich in Al_2O_3 and FeO and poor in K_2O (e.g., Turner, 1968). In the rocks of interest of this study, staurolite mainly occurs in highly aluminous bulk composition layers, showing strong alteration, and numerous ilmenite or quartz inclusions.

On the other hand, many petrologists would attribute the rare development of staurolite as compared with garnet, biotite and kyanite to a more restricted P-T range (Deer et al., 1992) or a limited range of oxygen fugacity (Ganguli, 1968). The stability field of staurolite is restricted roughly to medium P-T conditions commonly associated with regional metamorphism resulting from crustal thickening during earlier orogenic stages (Mezger, 2010).

Although staurolite-bearing rocks have a general composition field in the AKF diagram, the various mineral assemblages are better represented in AFM diagrams in which molecular proportions of FeO and MgO are considered as separate components (Lal and Shukla, 1970). To calculate the plotting parameters for the AFM diagram, we assume A = [Al_2O_3-$3K_2O$], F = [FeO], and M = [MgO]. Using these parameters, it is possible to grid off the AFM diagram with the vertical scale represented by the normalized values for the A parameter as [Al_2O_3-$3 K_2O$]/[Al_2O_3-$3K_2O$+FeO+MgO] and the horizontal position based on the ratio of MgO/(FeO+MgO). These values were obtained after converting the bulk rock chemistry data to molecular proportions (Figure 6).
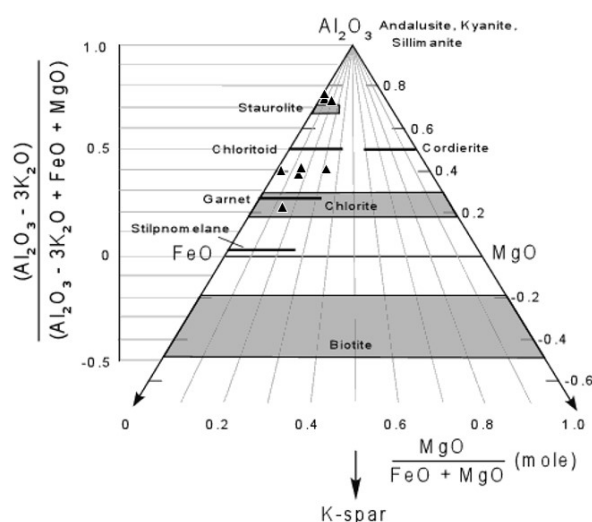

Figure 6. Bulk rock chemistry of staurolite-bearing rocks plotted on a AFM projection plane as black triangles. Adapted and modified after http://www.tulane.edu/~sanelson/eens212/triangular_plots_metamophic_petrology.htm

The staurolite-bearing metapelitic rocks of the Silgará Formation, which contain garnet, fall close to the three-phase field of biotite-garnet-staurolite (+quartz+muscovite) and have only a small range of FeO/MgO ratios. Plagioclase is ignored by the diagram (CaO is not plotted), but we can resolve biotite and garnet because they clearly have different compositions in the AFM plot. Because the garnet structure readily takes in Ca, and especially Mn, almandine garnet is stabilized beyond the range of conditions of bulk composition represented in the diagram. It is thus possible that the presence of sufficient Mn stabilizes garnet as a very common phase in the assemblage biotite- staurolite-Al_2SiO_5, and then the occurrence of garnet in the staurolite-bearing pelites may be related to high Mn content of the rock. In the AFM diagram, the analyses of these rocks show that they have a high Al_2O_3/(FeO+MgO) ratio (between 0.2 and 0.8). Further, they show a relatively variable FeO/MgO ratio, although they are restricted to low FeO/MgO ratio (between 0.0 and 0.4). Therefore, the bulk composition field of these rocks migrates towards the lower FeO/MgO side in the AFM diagram.
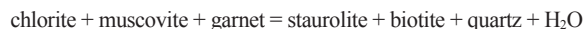
7. Discussion on staurolite-forming and -breakdown reactions (Figure 7)

Mineral chemistry and textural evidence shows that the Fe-rich staurolite in the metapelitic rocks of the Silgará Formation are involved in producing and consuming reactions. As follows, we discuss several reactions:

According to Bucher and Frey (1994), staurolite forms under greenschist facies conditions by continuous reactions such as:

chlorite + muscovite = staurolite + biotite + quartz + H_2O
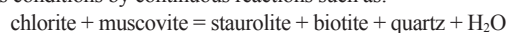
and discontinuous reactions such as:

chlorite + muscovite + garnet = staurolite + biotite + quartz + H_2O

However, Spear (1993) does not include quartz in the reaction products and, therefore, the growth of staurolite was accompanied by decomposition of garnet and continued decomposition of chlorite probably occurred by the reaction:

garnet + chlorite + muscovite = staurolite + biotite + H_2O

Ríos and Takasu (1999) consider that at the staurolite isograd, X_{grs} increases with increasing temperature, which is difficult to determine taking into account that garnet tends to be resorbed back to higher X_{grs} concentrations as staurolite grows. However, according to Ríos et al. (2003) after the maximum pressure conditions (P_{peak}), pressure does not remain constant, according to the chemical zoning of X_{grs} in garnet from the staurolite zone, which suggests a P_{peak} of metamorphism during garnet growth as suggested by Ríos and Takasu (1999).

The diagnostic mineral assemblage for the staurolite metamorphic zone is staurolite + garnet + biotite + muscovite + chlorite + plagioclase + quartz.
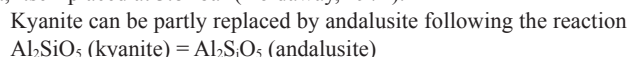
Staurolite growth is thus either syn- or post-tectonic with respect to the tectonic transport of the Silgará Formation metapelitic rocks. Garnet is sometimes found as inclusions within the staurolite poikiloblasts, which indicates that the rock from the staurolite zone first crossed a garnet-in reaction.

With increasing temperature, staurolite becomes unstable and reacts to produce garnet, biotite and kyanite by the following reaction

staurolite + muscovite + quartz = garnet + biotite + Al_2SiO_5 (kyanite) + H_2O
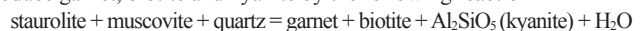
However, this reaction, which promotes the disappearance of staurolite also coincides with the appearance of kyanite (at pressure greater than about 2.5 kbar), and if we were to encounter this reaction in the field, it could be used to define the kyanite isograd.
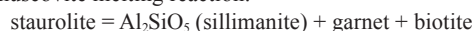
The occurrence of andalusite and sillimanite in these rocks can be associated to a superimposed low-P/high-T thermal event, although the presence of these polymorphs implies pressure below the Al_2SiO_5 triple point, itself placed at 3.8 kbar (Holdaway, 1971).

Kyanite can be partly replaced by andalusite following the reaction

Al_2SiO_5 (kyanite) = $Al_2S_iO_5$ (andalusite)

According to Yardley (1989), staurolite can be consumed by reactions, which generate sillimanite, such as

staurolite + muscovite + quartz = Al_2SiO_5 (sillimanite) + biotite + H_2O

and

staurolite + muscovite + quartz = Al_2SiO_5 (sillimanite) + garnet + biotite + H_2O

According to Spear (1993), the staurolite-out reaction occurs near the muscovite melting reaction:

staurolite = Al_2SiO_5 (sillimanite) + garnet + biotite

and, in this case, muscovite and quartz are not considered as reactants. This reaction would explain the highly resorbed staurolite. The occurrence of sillimanite and biotite rimming garnet suggest the dissolution of garnet by the continuous reaction:

garnet + Kfeldspar + melt = biotite + Al_2SiO_5 (sillimanite) (Spear et al.,1999)

This reaction also helps to explain the absence of K-feldspar. From these constraints, it is proposed that pelitic schists reached peak P-T conditions of 675-850 oC and 4-8 kbar. In the absence of muscovite, Yardley (1989) considers the following reaction

staurolite + quartz = Al_2SiO_5 (sillimanite) + garnet + H_2O
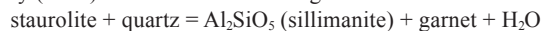
The reactions involving muscovite take place at a lower grade than the staurolite + quartz reaction (Bucher and Frey, 1994), so staurolite can persist to higher grades in muscovite-free assemblages, such as those in the Silgará Formation pelitic schists. Within the staurolite-bearing rocks of the Santander Massif, domains with abundant sillimanite have very little staurolite, with the relics that remain containing less Zn than in the sillimanite-free domains. Reactions such as those above have presumably consumed the Zn-poor staurolite and generated sillimanite. At this respect, we consider that the formation of sillimanite can be probably associated to a thermal event which has been recently registered the authors in several parts of the Santander Massif due to the emplacement of intrusive rocks. According to Foster and Dutrow (2010),

the nucleation of staurolite is controlled by two fundamental reactions: the stable reaction garnet + chlorite + muscovite = staurolite + biotite in regions that have equilibrated with garnet, and the metastable reaction chlorite + muscovite = staurolite + biotite in regions that have not equilibrated with garnet, and at 4 kbar, this reaction is overstepped first about 10 ºC below the stable reaction for a typical pelite composition, suggesting the metastable reaction may be an important control on staurolite nucleation and growth in these environments. In this study, we have observed textural features involving garnet and staurolite that can support this hypothesis.

Staurolite porphyroblasts (with inclusions of quartz and ilmenite) are corroded by fine grained aggregates of muscovite or muscovite + biotite that form thick coronas. The replacements also progress along fractures within staurolite, suggesting the presence of a fluid phase during replacement. Foster (1981) determined that muscovite and biotite pseudomorphs after staurolite formed as a result of sillimanite nucleation that sets up chemical potential gradients between the growing sillimanite, pre-existing staurolite, and the rock matrix of biotite, muscovite, plagioclase, quartz, ilmenite, and garnet. Staurolite is replaced by aggregates of muscovite. Muscovite replacement of staurolite becomes more prominent approaching the sillimanite zone, as the staurolite becomes unstable concurrent with the nucleation and growth of sillimanite (Whittington, 2006). However, a much simpler explanation is a retrograde reaction. Within these replacements, staurolite appears as fine xenomorphic grains that are often arranged in optical continuity, indicating that they are relicts of larger porphyroblasts.
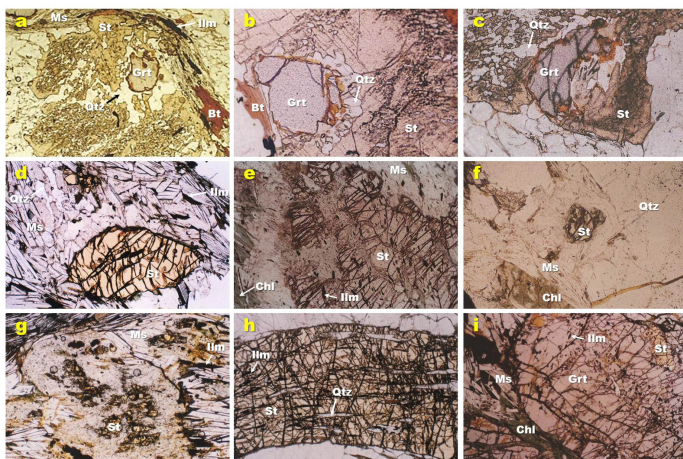

Figure 7. Reaction textures involving staurolite. (a)-(c) Relicts of garnet included in late staurolite porphyroblasts. (d) Highly corroded relicts of staurolite in contact with muscovite of the matrix. (e) Resorption of staurolite by sericite and muscovite, developing reaction rims around staurolite. (f) Highly corroded relict of staurolite in prograde muscovite. (g) Several corroded relict of staurolite enclosed by a very fine-grained aggregate of sericite (h) Poikiloblastic staurolite porphyroblast with oriented inclusions of quartz and ilmenite. (i) Relicts of staurolite in garnet porphyroblast.

8. Conclusions

Fe-rich staurolite in pelitic schists of the Silgará Formation at the Santander Massif (Colombian Andes) represent a very interesting index mineral for the reconstruction of the tectono-metamorphic evalution of this geological unit. Field occurrence and textural relations of staurolite with other mineral phases, as well as microstructural evidence observed in the investigated metapelites, reveal that these rocks underwent (1) prograde metamorphism during a complex polyphase deformation suggested by several foliations, as well as inclusion trails in staurolite porphyroblasts and (2) extensive retrograde metamorphism after the P_{peak}. With increasing metamorphic conditions, the protoliths of the staurolite-bearing metapelites were tectonically transported and buried to its maximum depth at the P_{peak}, (in the staurolite zone) which is attributed to crustal shortening and thickening accompanied by deformation, which produce, respectively, a slaty cleavage S_i and a crenulation

cleavage S_e associated with thrusting. Mineral chemistry along with textural relations was very useful to determine the staurolite-forming reactions in the Silgará Formation metapelites. Initially, staurolite (+ biotite + H_2O) formed as a product of the breakdown of the assemblage garnet + chlorite + muscovite. After the P_{peak}, these rocks experienced decompression, new mineral growth and movement strain-slip cleavages during a late deformation. In this study, we consider that the occurrence of andalusite and sillimanite (fibrolitic variety) as late mineral phases can be attributed to a thermal event superimposed to the regional metamorphism. Then, metapelites were affected by cooling accompanied by retrograde metamorphism as suggested by several rehydration reactions that often do not terminate and preserved relic mineral assemblages from the least hydrated states. The retrograde reactions may be associated to the infiltration of H_2O-rich fluids circulated along planes of discontinuity in metapelites of the Silgará Formation. Staurolite probably was consumed by reactions which generate Al_2SiO_5 (+biotite ± garnet + H_2O), which include as reactants staurolite + muscovite + quartz.

References

Banks, P., Vargas, R., Rodríguez, G.I., and Shagam, R. 1985. Zircon U-Pb ages from orthogneiss, Pamplona, Colombia. VI Congreso Latinoamericano de Geología, Bogotá. Resúmenes.

Bell, T.H., and Welch, P.W., 2002. Prolonged Acadian orogenesis: revelations from foliation intersection axis (FIA) controlled monazite dating of foliations in porphyroblasts and matrix. American Journal of Science, 302(7): 549-581.

Bucher, K., and Frey, M. 1994. Petrogenesis of Metamorphic Rocks: Complete Revision of Winkler's Textbook, Springer-Verlag, Berlín, 319 p.

Castellanos, O., Ríos, C., and Takasu, A. 2008. A new approach on the tectonometamorphic mechanisms associated with P–T paths of the Barrovian-type Silgará Formation at the Central Santander Massif, Colombian Andes. Earth Sciences Research Journal (Universidad Nacional de Colombia), 12: 125-155.

Deer, W.A., Howie, R.A., and Zussman, J. 1992. An Introduction To The Rock-Forming Minerals, Longman, London, 696p.

Dörr, W., Grösser, J., Rodriguez, G., and Kramm, U. 1995. Zircon U-Pb age of the Páramo Rico tonalite-granodiorite, Santander Massif (Cordillera Oriental, Colombia) and its geotectonic significance. Journal of South American Earth Sciences, 8(2): 187-194.

Foster, Jr, C.T., and Dutrow B.L. 2010. Controls on porphyroblast nucleation in high-grade metapelites. GeoCanada: Working with the Earth, Alberta. Technical Program Abstracts.

Foster, Jr, C.T. 1981. A thermodynamic model of mineral segregations in the lower sillimanite zone near Rangeley, Maine. American Mineralogist, 66: 260-277.

Ganguly, J. 1968. Analysis of the stabilities of chloritoid and staurolite and some equilibria in the system FeO-Al2O3-SiO2-H2O-O2. American Journal of Science, 266: 277-298.

García, C.A., Ríos, C.A., and Castellanos, O.M. 2005. Medium-pressure metamorphism in the central Santander Massif, Eastern Cordillera, Colombian Andes: constraints for a collision model. Boletín de Geología, 27: 43-68.

Goldsmith, R., Marvin, R., and Mehnert, H. 1971. Radiometric ages in the Santander Massif, eastern Cordillera, Colombian Andes. U.S. Geological Survey Professional Paper, 750-D: D41-D49.

University, Matsue (Japan), 150pp.

Ríos, C., and Takasu, A. 1999. Chemical zoning of garnet from the low-grade metamorphic rocks of the Silgará Formation, Santander Massif, Eastern Cordillera (Colombian Andes). Geosciences Reports of Shimane University, 18: 97-107.

Ríos, C.A., García, C.A., and Takasu, A. 2003. Tectono-metamorphic evolution of the Silgará Formation metamorphic rocks in the southwestern Santander Massif, Colombian Andes. Journal of South American Earth Sciences, 16: 133-154.

Ríos, C.A., Castellanos, O.M., Gómez, S., and Avila, G. 2008. Petrogenesis of the metacarbonate and related rocks of the Silgará Formation, central Santander Massif, Colombian Andes: An overview of a "reaction calcic exoscarn". Earth Sciences Research Journal (Universidad Nacional de Colombia), 12: 72-106.

Sanislav, I.V., and Shah, A.A. 2010. The Problem, Significance and Implications for Metamorphism of 60 Million Years of Multiple Phases of Staurolite Growth. Journal of the Geological Society of India, 76: 384-398.

Spear, F. 1993. Metamorphic phase equilibria and pressure-temperature-time paths, Monograph Series, Mineralogical Society of America, Washington, DC, 799pp.

Spear, F.S., Kohn, M.J., and Cheney, J.T. 1999. P-T paths from anatectic pelites. Contributions to Mineralogy and Petrology, 134: 17-32.

Turner, F.J. 1968. Metamorphic Petrology, McGraw-Hill, New York, 403p.

Ward, C.M. 1984. Magnesium staurolite and green chromian staurolite from Fiordland, New Zealand. American Mineralogist, 69: 531-540.

Ward, D.E., Goldsmith, R., Cruz, B.J., Jaramillo, C.L., and Vargas, L.R., 1970. Mapa Geológico del Cuadrángulo H-13, Pamplona, Colombia. Ingeominas.

Ward, D.E., Goldsmith, R., Cruz, B.J., Jaramillo, C.L., and Restrepo, H., 1973. Geología de los Cuadrángulos H-12, Bucaramanga y H-13, Pamplona, Departamento de Santander. U.S. Geological Survey e Ingeominas. Boletín Geológico XXI(1-3), 1-132.

Whittington, J.K. 2006. Muscovite pseudomorphs after staurolite as a record of fluid infiltrating during prograde metamorphism. Unpublished MSc Thesis, Louisiana State University, Baton Rouge (USA), 119pp.

Yardley, B. 1989. An Introduction to Metamorphic Petrology, Longman, Harlow, 248p.